

ISSN: 0095-8972 (Print) 1029-0389 (Online) Journal homepage: <http://www.tandfonline.com/loi/gcoo20>

New salen-type manganese(III) Schiff base complexes derived from meso-1,2-diphenyl-1,2-ethylenediamine: In vitro anticancer activity, mechanism of action, and molecular docking studies

Maryam Damercheli, Davood Dayyani, Mahdi Behzad, Bitra Mehravi & Mehdi Shafiee Ardestani

To cite this article: Maryam Damercheli, Davood Dayyani, Mahdi Behzad, Bitra Mehravi & Mehdi Shafiee Ardestani (2015) New salen-type manganese(III) Schiff base complexes derived from meso-1,2-diphenyl-1,2-ethylenediamine: In vitro anticancer activity, mechanism of action, and molecular docking studies, *Journal of Coordination Chemistry*, 68:9, 1500-1513, DOI: [10.1080/00958972.2015.1027697](https://doi.org/10.1080/00958972.2015.1027697)

To link to this article: <http://dx.doi.org/10.1080/00958972.2015.1027697>




View supplementary material 



Accepted author version posted online: 09 Mar 2015.
Published online: 09 Apr 2015.



Submit your article to this journal 



Article views: 150



View related articles 



View Crossmark data 



Citing articles: 1 View citing articles 



New salen-type manganese(III) Schiff base complexes derived from *meso*-1,2-diphenyl-1,2-ethylenediamine: *In vitro* anticancer activity, mechanism of action, and molecular docking studies

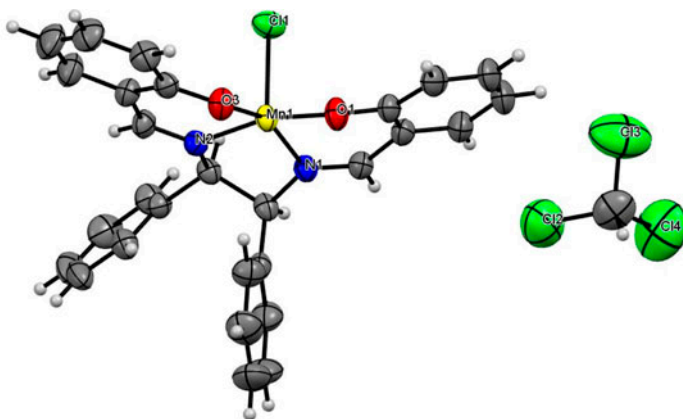
MARYAM DAMERCHELI[†], DAVOOD DAYYANI[†], MAHDI BEHZAD^{*†},
BITA MEHRAVI[‡] and MEHDI SHAFIEE ARDESTANI^{*§}

[†]Department of Chemistry, Semnan University, Semnan, Iran

[‡]Faculty of Advanced Technology in Medicine, Department of Medical Nanotechnology, Iran
University of Medical Sciences, Tehran, Iran

[§]Faculty of Pharmacy, Department of Radiopharmacy, Tehran University of Medical Sciences,
Tehran, Iran

(Received 4 December 2014; accepted 18 February 2015)



A series of new Mn(III) Schiff base complexes of a salen type ligand with general formula MnCIL^x were synthesized, characterized and tested for anticancer activity. The complexes showed considerable activity against the studied cell lines.

*Corresponding authors. Email: mbehzad@semnan.ac.ir, mahdibehzad@gmail.com (M. Behzad); shafieeardestani@sina.tums.ac.ir, shafieeardestani@gmail.com (M. Shafiee Ardestani)

Four new manganese(III) Schiff base complexes (**1–4**) were synthesized and characterized. The complexes have general formula $[\text{MnCIL}^x]$ in which L represents a Schiff base ligand derived from condensation of *meso*-1,2-diphenyl-1,2-ethylenediamine with salicylaldehyde or its 3-OMe-, 5-Br-, or 5-OMe-derivatives ($x = 1–4$, respectively). The crystal structure of $[\text{MnCIL}^1]$ (**1**) was characterized by X-ray crystallography. The *in vitro* anticancer activity of these complexes was evaluated by MTT and apoptosis assays against human breast (MCF-7) and liver (Hep G2) cancer cells. The complexes exhibited considerable antiproliferative activity against both cell lines ($\text{IC}_{50} = 10.8–21.02 \mu\text{M}$) comparable to cis-platin, except **4** (MCF-7). The highest activity was found for **1** with IC_{50} values of $13.62 \mu\text{M}$ (MCF-7) and $10.8 \mu\text{M}$ (Hep G2). Flow cytometry experiments showed that **1** induced apoptosis on MCF-7 tumor cell line. Docking simulations using AUTODOCK were also carried out. The results showed that all complexes fitted into the minor groove region of DNA.

Keywords: Schiff base; Mn(III); Anti-cancer; Molecular docking

1. Introduction

Metal-based anticancer drugs, such as cis-platin and its analogs, have received attention in cancer chemotherapy [1]. However, clinical problems like high toxicity, resistance to the drug, or unwanted side-effects have limited their use [2, 3]. In this regard, scientists have focused their attention to develop other classes of metal-based compounds, with the hope of finding less toxic and more effective anticancer drugs and also finding novel modes of DNA interactions [4–8]. DNA is a well-established pharmacological target of metal-based anticancer drugs and knowledge of the DNA-drug binding mode is very important for rational drug design [9, 10]. Schiff base complexes are among the most widely studied class of such compounds, thanks to their ease of synthesis and the possibility of the adjustment of their electronic and steric characteristics. Salen-type Schiff bases are the most widely studied ligands in this family of compounds [11]. For most transition metals, the corresponding salen complex is reported [11]. Salen-metal complexes have very high binding constants in the range of $\log K > 20$ [12, 13] which has made them suitable for several purposes. Coordination chemistry of manganese has been investigated for applications such as catalysis, antibacterial and anti-fungal drugs, catalytic activity for specific DNA and RNA cleavage reactions, and many other applications [14–19]. There is interest in the chemistry of Mn(III) complexes with Schiff base ligands for biological studies; hence, we are interested in studying the anticancer activity of a series of new Mn(III) salen-Schiff base complexes. We have previously synthesized and characterized different transition metal complexes of salen-type Schiff base ligands, especially those derived from *meso*-1,2-diphenyl-1,2-ethylenediamine, and have studied their catalytic and biological properties [20–30]. In continuation of our previous studies, we report the synthesis and characterization of four new Mn(III) complexes with Schiff bases of general formula $[\text{MnCIL}^x]$ ($x = 1–4$). L is a Schiff base derived from the condensation of *meso*-1,2-diphenyl-1,2-ethylenediamine with different salicylaldehyde derivatives (scheme 1). The *in vitro* anticancer activities of these complexes were evaluated by MTT assay with two tumor cell lines, human breast (MCF-7), and liver (Hep G2) cancer cells. Flow cytometry was performed for cell death analysis. The relationship between the chemical structure of the complexes and their biological activity was also described. To obtain *in silico* knowledge of DNA-binding mode of the synthesized complexes, docking simulations using AUTODOCK were also carried out. The results showed that **1** could act as a promising compound for further structure optimization and *in vivo* evaluation, owing to its interesting biological activity against cancer cells.

2. Experimental

2.1. Materials and methods

All chemicals were purchased from commercial sources and used as received. *Meso*-1,2-diphenyl-1,2-ethylenediamine [31] and H_2L^n ($n = 1-4$) [20–23] were synthesized as described. Melting points were obtained on a Thermoscientific 9100 apparatus. IR spectra were obtained as KBr plates using a Bruker FTIR instrument. UV-vis spectra were obtained on a Shimadzu UV-1650PC spectrophotometer in DMSO. A Metrohm 757VA computerized instrument was employed to obtain cyclic voltammograms. X-ray data were collected at room temperature with a Bruker APEX II CCD area-detector diffractometer using $Mo K_\alpha$ radiation ($\lambda = 0.71073 \text{ \AA}$). Human breast cancer cells (MCF-7) and human liver cancer cells (Hep-G2) were obtained from the National cell Bank of Pasteur Institute of Iran. The cells (3×10^3 per well) were grown in RPMI 1640 supplemented with 10% fetal bovine serum and antibiotics (penicillin-streptomycin) at 37°C and 5% CO_2 . The absorbance of purple formazone of each well was measured using BioTek's absorbance microplate reader at 450 nm (ELX800; BioTek Instruments Inc., Winooski, VT, USA). The apoptotic studies were carried out using a flow cytometer (FAC Scan Cytometer equipped with Cell Quest Software. Becton Dickinson Immune cytometry System BD Biosciences, San Jose, CA, USA), by counting 30,000 events, and data were analyzed using WinMDI software.

2.2. Synthesis of the complexes

The complexes were synthesized via the equimolar reaction between H_2L^{1-4} and $Mn(OAc)_2 \cdot nH_2O$ in ethanol. In a typical experiment, a solution of 0.50 g (1.2 mmol) of H_2L^1 in 30 mL of ethanol was heated to 60°C and vigorously stirred. Then, a solution of 0.29 g $Mn(OAc)_2 \cdot nH_2O$ (1.2 mmol) in 20 mL of ethanol was added dropwise. The color of the solution gradually turned brown. The reaction mixture was heated for 1 h and then lithium chloride was added. The reaction mixture was refluxed for 2 h and the solution was allowed to cool to room temperature. The solvent was removed to dryness using a rotary evaporator. The brown solid was collected, washed with water and dichloromethane, and air-dried. Recrystallization from dichloromethane yielded pure crystals of the target complex in good yield. Scheme 1 shows the schematic representation of the synthetic procedure for the preparation of the ligands and complexes, and spectroscopic and analytical data for the complexes are collected in table 1.

2.3. X-ray crystallography

Diffraction data were collected at room temperature with a Bruker APEX II CCD area-detector diffractometer using MoK_α radiation ($\lambda = 0.71073 \text{ \AA}$). Data collections, cell refinements, data reductions, and absorption corrections were performed using multi-scan methods with Bruker software [32]. The structures were solved by direct methods using SIR2004 [33]. The non-hydrogen atoms were refined anisotropically by the full-matrix least-squares method on F^2 using SHELXL [34]. All hydrogens were placed at calculated positions and constrained to ride on their parent atoms. Details concerning collections and analyses are reported in tables 2 and 3.

2.4. Cyclic voltammetry

A Metrohm 757 VA computrace instrument was employed to obtain cyclic voltammograms in DMSO solutions at room temperature (25 °C), and 0.1 M tetrabutylammonium hexafluorophosphate (TBAH) as supporting electrolyte under N₂. Glassy carbon working electrode, a reference Ag/AgCl electrode, and an auxiliary Pt electrode were used. The values for the redox potential are presented in table 4 and are corrected against Fc⁺⁰.

2.5. Biological tests

2.5.1. Cell lines and growth conditions. 3-(4,5-Dimethylthiazol-2-yl)-2,5-diphenyltetrazoliumbromide (MTT)-based cell proliferation assay was used to determine cytotoxicity of the synthesized complexes. For evaluation of growth inhibition tests, the cells were incubated with various amounts of the complexes (0–80 μM) in a 96-well microplate for 24 h using unlabeled cells as control. Prior to this, stock solutions of the complexes were prepared by dissolving the complexes in 1 mL of DMSO and diluting in RPMI medium, followed by addition of 100 μL of each complex to the wells to obtain a final concentration ranging between 0 and 80 μM. Each concentration was tested in triplicate. After incubation for the indicated intervals, 20 μL of a MTT solution in PBS (2 mg mL⁻¹) was added to each well and the plates were incubated for 2 h at 37 °C. Percentage of survival was calculated as a fraction of the negative control. The half-maximal inhibitory concentration (IC₅₀) values for the inhibition of cell growth were obtained from the dose-response curve with Pharm software [35].

Table 1. Spectroscopic and analytical data for **1–4**.

Complex	Yield (%)	Selected IR (cm ⁻¹)	UV-vis, nm (ε, M ⁻¹ cm ⁻¹)	Elem. Anal. Calcd (found)
[MnCIL ¹]·CHCl ₃	75.4	1604(ν _{C=N})	287 (22,600), 320 (12,100), 405 (5100)	C: 55.39 (55.47); H: 3.66 (3.75); N: 4.46 (4.35)
[MnCIL ²]·CH ₂ Cl ₂	89.5	1596(ν _{C=N})	272 (17,700), 335 (13,200), 422 (5300)	C: 56.88 (56.97); H: 4.28 (4.39); N: 4.28 (4.19)
[MnCIL ³]·CH ₂ Cl ₂	62.4	1608(ν _{C=N})	268 (27,100), 332 (9300), 412 (3100)	C: 46.21 (46.35); H: 2.92 (3.02); N: 3.72 (3.65)
[MnCIL ⁴]·CH ₂ Cl ₂	84.9	1598(ν _{C=N})	267 (27,600), 350 (9400), 468 (5400)	C: 56.88 (57.01); H: 4.28 (4.35); N: 4.28 (4.17)

Table 2. Selected bond lengths and angles for [MnCIL¹]·CHCl₃.

Bond lengths (Å)		Bond angles (°)	
Mn(1)–O(1)	1.863(2)	O(1)–Mn(1)–Cl(1)	99.46(9)
Mn(1)–O(3)	1.887(2)	O(3)–Mn(1)–Cl(1)	102.49(9)
Mn(1)–N(1)	1.975(3)	N(1)–Mn(1)–Cl(1)	102.39(9)
Mn(1)–N(2)	1.987(2)	N(2)–Mn(1)–Cl(1)	92.86(8)
Mn(1)–Cl(1)	2.3664(15)	O(1)–Mn(1)–O(3)	91.86(10)
		O(1)–Mn(1)–N(1)	89.95(11)
		O(1)–Mn(1)–N(2)	166.29(11)
		O(3)–Mn(1)–N(1)	154.40(11)
		O(3)–Mn(1)–N(2)	91.33(10)
		N(1)–Mn(1)–N(2)	81.48(10)

Table 3. Crystal data, data collection, and structure refinement parameters for [MnCIL¹]-CHCl₃.

Crystal data	[MnCIL ¹]
Empirical formula	C ₂₉ H ₂₃ Cl ₄ MnN ₂ O ₂
Formula weight	628.23
<i>T</i> (K)	298(2)
λ (Å)	0.71073
Crystal system	Triclinic
Space group	<i>P</i> − <i>I</i>
Unit cell dimensions (Å, °)	
<i>a</i> (Å)	10.601(2)
<i>b</i> (Å)	10.850(2)
<i>c</i> (Å)	114.604(3)
α (°)	76.76(3)
β (°)	172.13(3)
γ (°)	63.44(3)
Volume (Å ³), <i>Z</i>	1421.7(6), 2
Calculated density (g cm ^{−3})	1.468
Absorption coefficient (mm ^{−1})	0.870
<i>F</i> (0 0 0)	640
θ range for data collection (°)	2.11–29.20
Limiting indices	−14 ≤ <i>h</i> ≤ 12, −14 ≤ <i>k</i> ≤ 14, −18 ≤ <i>l</i> ≤ 19
Data/restraints/parameters	7592/0/343
Total reflections	15,025
Unique reflections (<i>R</i> _{int})	7592 (<i>R</i> (int) = 0.0599)
Completeness	98.6% (θ = 29.20)
Refinement method	Full-matrix least squares on <i>F</i> ²
Goodness-of-fit on <i>F</i> ²	0.989
Final <i>R</i> index [<i>I</i> > 2σ(<i>I</i>)]	<i>R</i> ₁ = 0.0599, <i>wR</i> ₂ = 0.1572
<i>R</i> index [all data]	<i>R</i> ₁ = 0.0986, <i>wR</i> ₂ = 0.1840
Largest difference peak and hole (e Å ^{−3})	0.731 and −0.597

2.5.2. Apoptosis-necrosis assay. The apoptosis was determined using an Annexin V-propidium iodide staining kit as per the manufacturer recommendations. For cell viability assay, the MCF-7 cell line (1 × 10⁵ cells per well) was incubated with the most potent agent (**1**) (2 μg mL^{−1}) in a 24-well micro-plate for 24 h with untreated cells as positive control. Each concentration was tested in duplicate [36].

2.5.3. Computational studies.

2.5.3.1. *Molecular modeling.* The structure models of the complexes were built by Hyperchem-8.0 [37]. Geometric optimization has been performed in a two-step procedure. Initially, these compounds underwent energy minimization by use of MM⁺ force field as implemented in Hyperchem. Semi-empirical method PM3 Hamiltonian with Unrestricted Hartree–Fock and RMS gradient of 0.01 kcal M^{−1} was then used for optimizing the full geometry of the complexes.

Table 4. Electrochemical data for the 10^{−3} M DMSO solutions of [MnCIL^x] complexes at scan rate 100 mV s^{−1}.

Complex	<i>E</i> ⁰ (mV)	<i>E</i> _c (mV)	<i>E</i> _a (mV)	Δ <i>E</i> (mV)
[MnCIL ¹]	−175	−217	−133	83
[MnCIL ²]	−140	−191	−89	101
[MnCIL ³]	−56	−109	−3	106
[MnCIL ⁴]	−199	−256	−142	113

2.5.3.2. Docking calculations. The rigid molecular docking studies were performed by using MGL tools 1.5.6 with Autogrid4 and Autodock4 [38]. The structure of B-DNA (PDB ID: 1BNA) was downloaded from protein data bank. Crystallographic water molecules were removed and polar hydrogens and kollman charges were added to the receptor. The grid size was set to $72 \times 96 \times 118$ point to covering whole receptor for blind dock with a grid spacing of 0.375. Lamarckian genetic algorithm was chosen to perform docking calculations. Default values for all other parameteres have been set.

3. Results and discussion

3.1. Synthesis and spectroscopic characterization of the complexes

The ligands were synthesized according to our previously reported method. The complexes were synthesized following a general route for the synthesis of Mn(III) complexes of salen-type tetradentate Schiff base complexes [39]. The complexes were stable both in the solid state and in solution. In IR spectra of salicylaldehyde derivatives, a strong peak corresponding to the carbonyl stretching vibration is usually observed at 1680 cm^{-1} . Upon condensation with *meso*-1,2-diphenyl-1,2-ethylenediamine to form azomethine or imine (C=N) functional group, these bands disappear and new bands corresponding to the stretch of the formed imines are observed at 1630 cm^{-1} . This new band is usually shifted to lower wavenumbers upon coordination to metal ions due to the backbone donation of electron density to the π^* molecular orbital of the imine [24]. In **1–4**, the bands corresponding to the stretching vibration of the azomethine functional groups were observed at $1600 \pm 10\text{ cm}^{-1}$, which is confirmative of the coordination of nitrogen to the metal center. In electronic spectra of the parent ligands, two intense bands at 260 and 300 nm were assigned to the $\pi \rightarrow \pi^*$ transitions of the aromatic rings and imines, respectively [24]. These bands were present in the UV-vis spectra of the complexes. The appearance of new bands above 400 nm with a very weak shoulder at higher wavelengths were assigned to metal-to-ligand charge transfers and *d–d* transitions, respectively, which are similar to previously reported closely related [Mn(salen)X] complexes [40]. Elemental analyses were also in agreement with the proposed structures.

3.2. X-ray crystallography

Figure 1 shows the ORTEP representation of $\text{MnCIL}^1 \cdot \text{CHCl}_3$ with the common atom numbering scheme. Selected bond lengths and angles are cited in table 2, and a summary of the crystallographic data is collected in table 3. The complex is neutral and Mn(III) is coordinated to an L^{2-} Schiff base and a Cl^- . The geometry around the metal center is a distorted square-based pyramidal where the N_2O_2 Schiff base ligand is coordinated at the basal plane of the pyramid from its two deprotonated phenol oxygens and two imino nitrogens. The metal center is located about 0.313 \AA above this basal plane. The N–Mn–Cl and O–Mn–Cl bond angles, which are larger than 90° , confirm this distortion (table 2). The observed Mn–N, Mn–O, and Mn–Cl bond lengths are in the range of previously reported similar complexes [41, 42]. The disposition of the Schiff base ligand in the crystal structure of this complex is not planar, giving a boat-shaped structure similar to some of the previously observed related complexes [43, 44]. The dihedral angle between the planes defined by the

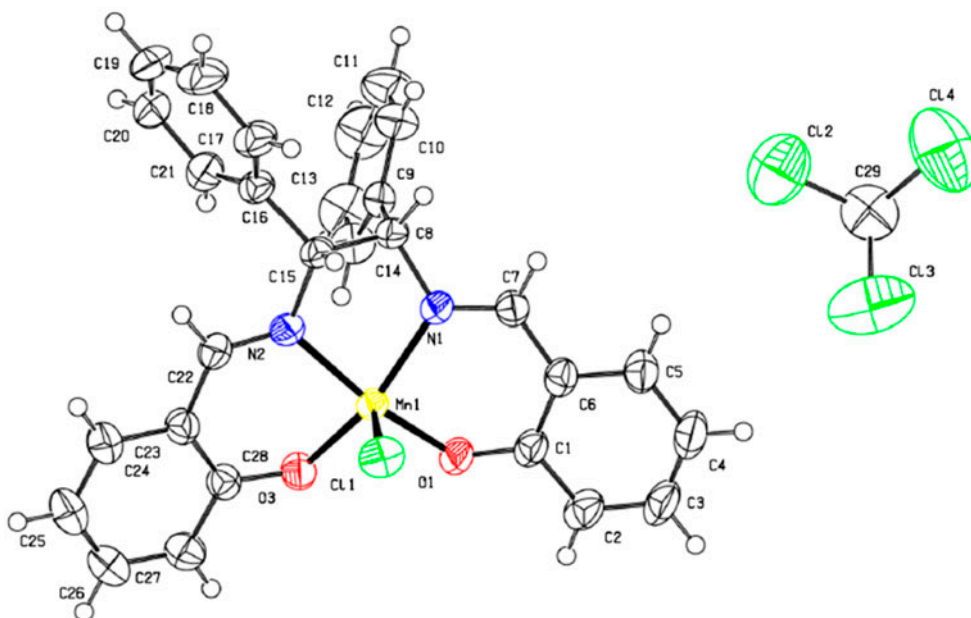


Figure 1. ORTEP representation of $[\text{Mn}(\text{CIL})^1] \cdot \text{CHCl}_3$. Displacement ellipsoids are drawn at 50% probability. Hydrogens are drawn at arbitrary radii.

two phenyl rings of the salicylaldehyde moiety is $33.71(2)^\circ$. No important hydrogen bond or π - π interactions were observed in the superstructure of the complex. The trigonality index, $\tau = (\varphi_1 - \varphi_2)/60$, where φ_1 and φ_2 are the two largest L-M-L angles of the coordination sphere, has been calculated. The value of $\tau = 0.20$ is close to the index of square-based pyramids, confirming the distorted square-based pyramidal structure around the metal center ($\tau = 0$ is the value for ideal square-based pyramids and $\tau = 1$ is the value for ideal trigonal bipyramidal structures [45]).

3.3. Cyclic voltammetry

Electrochemical behavior of the complexes was studied by cyclic voltammetry in the potential range +1.5 to -1.5 V. DMSO was used as solvent and 0.1 M TBAH as supporting electrolyte. The experiments were conducted at room temperature under N_2 using a glassy carbon working electrode, a platinum auxiliary electrode, and an Ag/AgCl reference electrode. The electrochemical data for the complexes are collected in table 4 and are corrected against $\text{Fc}^{+/0}$. The cyclic voltammograms of the $[\text{Mn}(\text{CIL})^x]$ complexes are shown in figure 2. The ligands were electro-inactive in the studied potential range [23]. In the cyclic voltammograms of the complexes, a quasi-reversible peak was observed for $[\text{Mn}^{\text{III}}(\text{CIL})^x] + 1e \rightarrow [\text{Mn}^{\text{II}}(\text{CIL})^x]$ process which is similar to those of previously reported similar complexes [40]. As shown in table 4, the presence of electron-withdrawing bromo-substitution in the para position of the phenoxo groups of the Schiff base ligand shifted the E^0 to more positive values while the methoxy-substitution in the para position shifted to more negative values. This could be rationalized from the fact that the more electron-withdrawing nature of the substituents destabilizes higher oxidation number Mn(III).

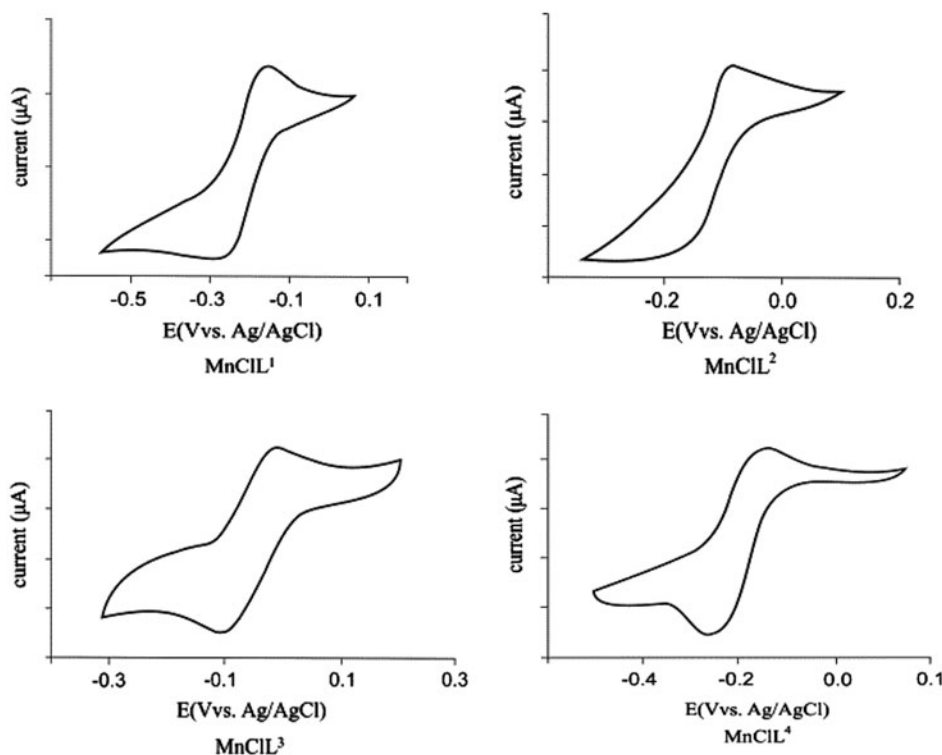


Figure 2. Cyclic voltammograms of the complexes in DMSO at 298 K and 100 mV s^{-1} scan rate.

3.4. Biological studies

3.4.1. Cytotoxic activity. The *in vitro* anticancer potential of **1–4** was established by monitoring their ability to inhibit cell growth by MTT assay [35]. Cytotoxic properties have been evaluated against two different human carcinoma cell lines MCF-7 and Hep-G2. Cis-platin was used as positive control to assess the cytotoxicity of the test compounds. $[\text{Mn}(\text{salen})\text{Cl}]$ and the ligands were also tested to obtain better structure-function insights. The ligands were almost inactive with IC_{50} values higher than $100 \mu\text{M}$. The obtained results showed that the synthesized complexes exhibited promising biological activity against both cell lines, which are almost as potent as the well-known anticancer drug cis-platin (table 5). The Hep-G2 cell line was more sensitive to these complexes. Compared to $[\text{Mn}(\text{salen})\text{Cl}]$, it was clear that the presence of the two phenyl rings of the diamine was important for cell toxicity. Comparison of the data for **1–4** showed that although the complexes did not show substantial difference in cell toxicity, complex **1** was the most active one. This shows that steric effect might play an important role in cell toxicity of these compounds. We tried to find electronic correlations with the cell toxicity, but in these complexes such electronic-function correlations were not found. More studies are necessary before a final conclusion. We are currently preparing other series of Mn(III) complexes with similar Schiff bases as ligands for further studies.

3.4.2. Apoptosis-necrosis analysis. The induced apoptosis effects of **1** were examined by performing Annexin V-FITC/PI staining to determine viable, early apoptotic, and late apoptotic cells. It is known that phosphatidylserine externalization is an early feature of apoptosis, which is Annexin V-positive. Viable cells did not bind to Annexin V or PI (lower left quadrant Q3), early apoptotic cells bound to Annexin V but excluded PI (lower right quadrant Q4), and late apoptotic cells were both Annexin V and PI positive (upper right quadrant Q2). The upper left quadrant Q1 contains dead cells [46, 47]. The results as depicted in figures 3 and S1 (see online supplemental material at <http://dx.doi.org/10.1080/00958972.2015.1027697>) show that **1** compared to the control could definitely promote cancer cell death through the activation of apoptosis pathway as it is indicated for FDA-approved anticancer drugs like cis-platin. As shown in figure 3, more than 43% of cells were dead through apoptosis mechanism.

3.4.3. DNA Molecular docking analysis. Molecular docking simulation is a well-documented computational tool to study the DNA-drug binding mode, in order to develop rational drug design and to predict the proper binding site of the target DNA mainly in a non-covalent mode [48]. Literature survey revealed that the metal complexes can interact with DNA through three non-covalent modes *viz.* intercalation, groove-binding, and electrostatic effects, and the effectiveness of these compounds depends on DNA-binding affinity of them. Among these modes, groove-binding plays an important role in the binding of the drug targeted to DNA [49, 50]. In our experiments, the main goal of this part of the work was to perform docking analysis of DNA-binding affinity of the synthesized complexes. Therefore, we studied the DNA-binding mode of these complexes to understand the preferred orientation and the type of interaction between the complexes and DNA. The energetically most favorable conformation of the docked pose (figures 4 and S2–S3) revealed that all complexes fitted into the minor groove region of DNA within G–C regions compared to A–T ones, and lead to van der Waals interactions and hydrophobic contacts with DNA functional groups which define the stability of the groove [51]. It is well known that, in contrast to major groove, small molecules preferentially interact with the minor groove due to little steric interference [52]. From the analysis of the docked structures

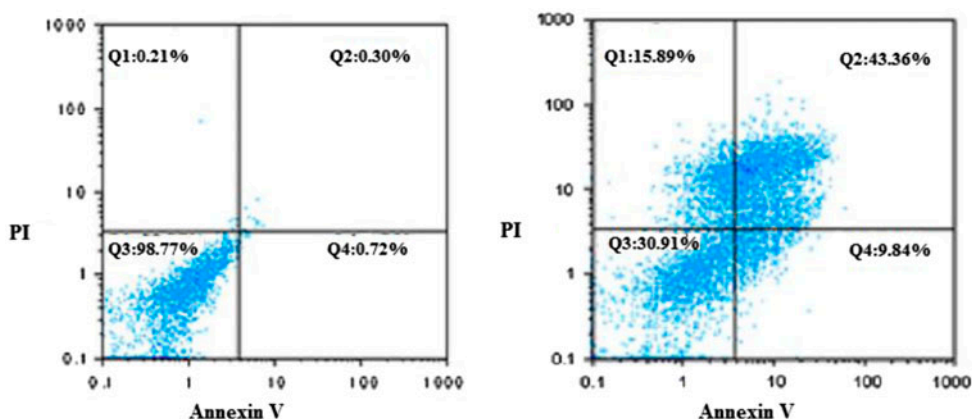


Figure 3. Flow cytometry data on the MCF-7 cells as control (left) and **1** (right).

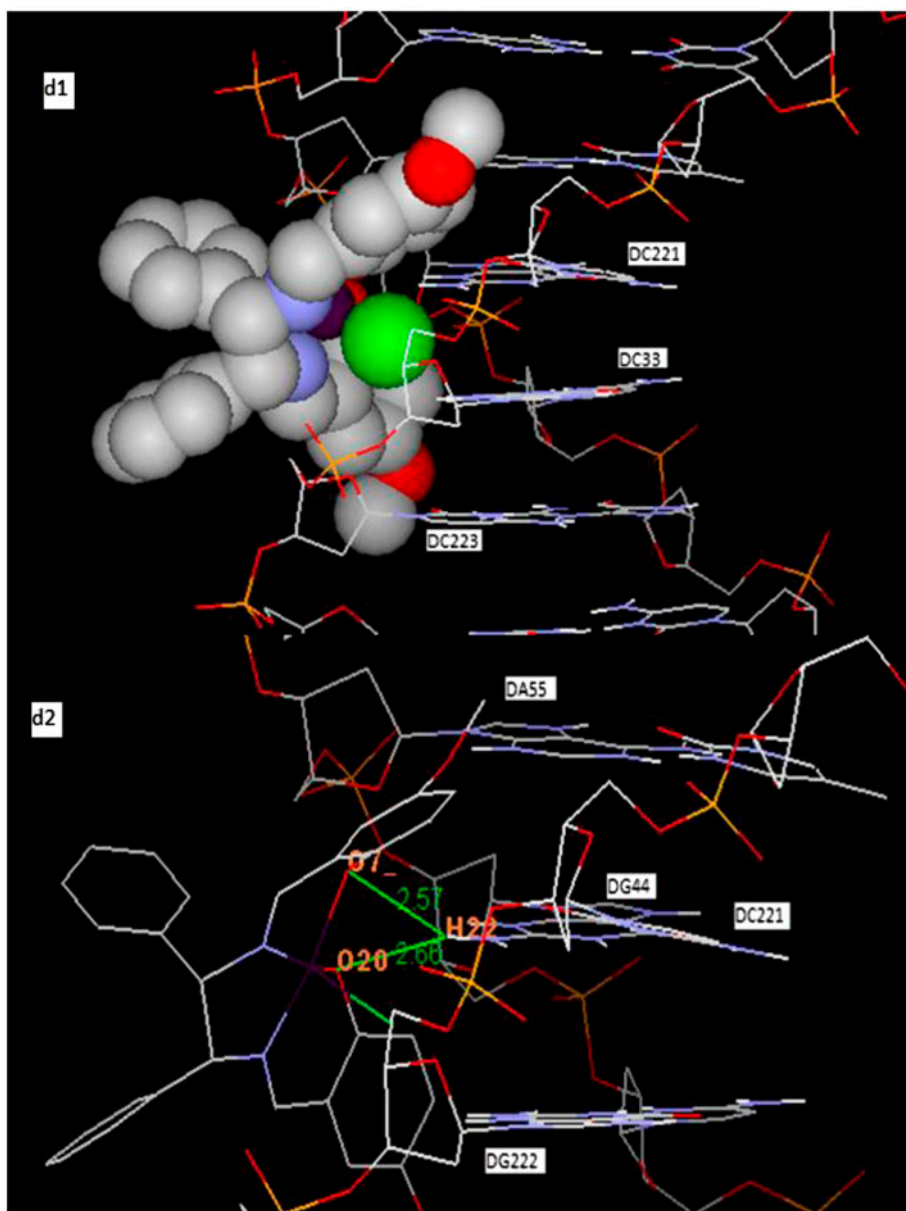


Figure 4. Molecular docked model (d1) and hydrogen bindings (d2) of **4** with DNA [dodecamer duplex of sequence d(CGCGAATTCGCG)2 (PDB ID: 1BNA)].

(figures 4 and S2–S3) we conclude the following remarks: (i) Complexes **1** and **4** were stabilized by at least one hydrogen bond between phenolic oxygen and the DNA bases, in addition to van der Waals interactions. The main characteristics of the predicted H-bindings to DNA for these complexes are listed in table 6. (ii) Complexes **1**–**3** were stabilized in binding pockets by adjusting one aromatic ring from each salicylaldehyde and diamine

Table 5. IC₅₀ values for 1–4 and cis-platin against MCF-7 (breast) and Hep-G2 (liver) cancer cells. SD is the standard deviations of the values. Cell viability assessed after 24 h of incubation.

Compound	IC ₅₀ (μM) ± SD	
	MCF-7	Hep-G2
L ^{1–4}	>100	>100
[MnCIL ¹]	14 ± 1	11 ± 2
[MnCIL ²]	16 ± 1	12 ± 1
[MnCIL ³]	16 ± 1	12 ± 2
[MnCIL ⁴]	21.0 ± 0.5	16 ± 1
[Mn(salen)Cl]	48.9 ± 0.5	35.2 ± 0.6
Cis-platin	20 ± 1	38.3 ± 0.7

Table 6. Hydrogen bonds among the complexes and DNA base pairs.

Complex	Hydrogen bonds	Distance (Å)	Angle (°)
1	O(20)···H(22)A : DG44	2.41	143.8
4	O(7)···H(22)A : DG44	2.57	140.5
	O(20)···H(22)A : DG44	2.66	160.2

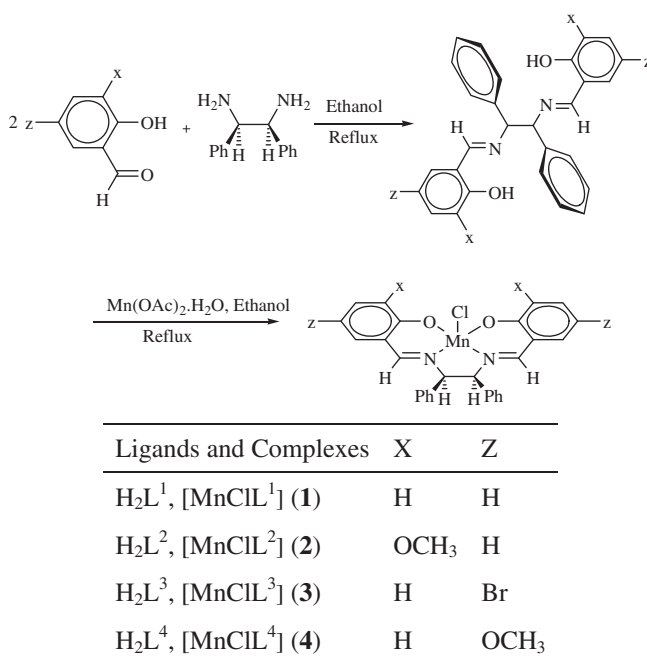
Table 7. Docking energy (kcal M^{−1}) for 1–4.

Complex	Vdw	Hb + desolv	Elec	ΔG	K _i (μM)
1	−6.67	−0.02	+0.16	−5.98	41.71
2	−7.58	−0.01	+0.15	−6.34	22.42
3	−7.33	0.00	+0.09	−6.69	12.48
4	−7.13	−0.25	−0.5	−6.78	10.74

Vdw: van der Waals energy.
Hb: hydrogen bonding energy.
Desolv: desolvation energy.
Elec: electrostatic energy.
ΔG: free energy of binding.
K_i: inhibition constant.

moieties that were partially intercalated into the minor groove and made favorable stacking forces with DNA bases, while **4** used both the aromatic rings of the salicylaldehyde moieties for intercalation. (iii) The methoxy-substituents were not involved in hydrogen bonding. (iv) Our results further showed that van der Waals interactions were dominant over other interactions (table 7) and became more important in the presence of the methoxy- and bromo-substituents, especially for the *x*-positions (scheme 1).

The resulting relative binding energies of docked **1–4** with DNA were found to be −5.98, −6.34, −6.69, and −6.78 kcal M^{−1}, respectively. These values are in the reverse order of the cytotoxicity results. Hence, it seems that the metal complexes do not reach the DNA target *in vitro* or, if they do reach the DNA, they must be easily removed by various DNA-repairing mechanisms [53]. Protein targets have also been implicated in the biological role of metal complexes [54] and it would appear that the complexes bind efficiently to proteins. These findings of molecular docking study prompted us to further study and explore the DNA-binding properties of synthesized complexes at experimental level.



Scheme 1. Synthetic procedure for the preparation of ligands and complexes.

4. Conclusion

Four new Mn(III) complexes with a series of salen type Schiff bases as ligands were synthesized and characterized. The *in vitro* anticancer activities of the complexes were evaluated. The complexes showed considerable anticancer activity against two human carcinoma cell lines. The anticancer activities of these complexes, as well as $[\text{Mn}(\text{salen})\text{Cl}]$, were compared to cis-platin. The complexes showed better anticancer activity compared to both cis-platin and $[\text{Mn}(\text{salen})\text{Cl}]$. For these complexes, the steric factors were more important than the electronic factors of Mn(III).

Supplementary material

CCDC 957350 contains the supplementary crystallographic data for MnClL^1 . These data can be obtained free of charge via <http://www.ccdc.cam.ac.uk/conts/retrieving.html>, or from the Cambridge Crystallographic Data Center, 12 Union Road, Cambridge CB2 1EZ, UK; Fax: (+44) 1223 336 033; or E-mail: deposit@ccdc.cam.ac.uk.

Disclosure statement

No potential conflict of interest was reported by the authors.

References

- [1] M.J. Hannon. *Pure Appl. Chem.*, **79**, 2243 (2007).
- [2] L. Kelland. *Nat. Rev. Cancer*, **7**, 573 (2007).
- [3] D. Wang, S.J. Lippard. *Nat. Rev. Drug Discov.*, **4**, 307 (2005).
- [4] N. Pravin, N. Raman. *Eur. J. Med. Chem.*, **85**, 675 (2014).
- [5] A. Sigel, H. Sigel (Eds.). *Metal Ions in Biological Systems, Metal Ions and Their Complexes in Medication*, Vol. 41, Marcel Dekker, New York (2004).
- [6] Y.L. Li, Z.W. Wang, P. Guo, L. Tang, R. Ge, S.R. Ban, Q.Y. Chai, L. Niu, Q.S. Li. *J. Inorg. Biochem.*, **133**, 1 (2014).
- [7] Z.D. Matović, E. Mrkalić, G. Bogdanović, V. Kojić, A. Meetsma, R. Jelić. *J. Inorg. Biochem.*, **121**, 134 (2013).
- [8] C. Shobha Devi, P. Nagababu, S. Natarajan, N. Deepika, P. Venkat Reddy, N. Veerababu, S.S. Singh, S. Satyanarayana. *Eur. J. Med. Chem.*, **72**, 160 (2014).
- [9] R. Manikandan, P. Viswnathamurthi. *Spectrochim. Acta, Part A*, **97**, 864 (2012).
- [10] L.N. Ji, X.H. Zou, J.G. Liu. *Coord. Chem. Rev.*, **216–217**, 513 (2001).
- [11] C. Baleizão, H. Garcia. *Chem. Rev.*, **106**, 3987 (2006).
- [12] A. Jancsó, Z. Paksi, S. Mikkola, A. Rockenbauer, T. Gajda. *J. Inorg. Biochem.*, **99**, 1480 (2005).
- [13] N.S. Venkataramanan, S. Prem Singh, S. Rajagopal, K. Pitchumani. *J. Org. Chem.*, **68**, 7460 (2003).
- [14] S. Amer, N. El-Wakiel, H. El-Ghamry. *J. Mol. Struct.*, **1049**, 326 (2013).
- [15] K. Ghosh, N. Tyagi, P. Kumar, U.P. Singh, N. Goel. *J. Inorg. Biochem.*, **104**, 9 (2010).
- [16] S. Mandal, A.K. Rout, A. Ghosh, G. Pilet, D. Bandyopadhyay. *Polyhedron*, **28**, 3858 (2009).
- [17] D. Moreno, V. Daier, C. Palopoli, J.-P. Tuchagues, S. Signorella. *J. Inorg. Biochem.*, **104**, 496 (2010).
- [18] X. Dong, Y. Li, Z. Li, Y. Cui, H. Zhu. *J. Inorg. Biochem.*, **108**, 22 (2012).
- [19] A.-N.M.A. Alaghaz, B.A. El-Sayed, A.A. El-Henawy, R.A.A. Ammar. *J. Mol. Struct.*, **1035**, 83 (2013).
- [20] Z. Abbasi, M. Behzad, A. Ghaffari, H. Amiri Rudbari, G. Bruno. *Inorg. Chim. Acta*, **414**, 78 (2014).
- [21] H. Iranmanesh, M. Behzad, G. Bruno, H. Amiri Rudbari, H. Nazari, A. Mohammadi, O. Taheri. *Inorg. Chim. Acta*, **395**, 81 (2013).
- [22] A. Ghaffari, M. Behzad, M. Pooyan, H. Amiri Rudbari, G. Bruno. *J. Mol. Struct.*, **1063**, 1 (2014).
- [23] O. Taheri, M. Behzad, A. Ghaffari, M. Kubicki, G. Dutkiewicz, A. Bezaatpour, H. Nazari, A. Khaleghian, A. Mohammadi, M. Salehi. *Transition Met. Chem.*, **39**, 253 (2014).
- [24] A. Ghaffari, M. Behzad, G. Dutkiewicz, M. Kubicki, M. Salehi. *J. Coord. Chem.*, **65**, 840 (2012).
- [25] D.M. Boghaei, A. Bezaatpour, M. Behzad. *J. Coord. Chem.*, **60**, 973 (2007).
- [26] M. Pooyan, A. Ghaffari, M. Behzad, H. Amiri Rudbari, G. Bruno. *J. Coord. Chem.*, **66**, 4255 (2013).
- [27] A. Bartyzel. *J. Coord. Chem.*, **66**, 4292 (2013).
- [28] Y.L. Sang, X.C. Li, W.M. Xiao. *J. Coord. Chem.*, **66**, 4015 (2013).
- [29] A. Aghmiz, N. Mostfa, S. Iksi, R. Rivas, M.D. González, Y. Díaz, F. El Guemmout, A. El Laghdach, R. Echarrí, A.M. Masdeu-Bultó. *J. Coord. Chem.*, **66**, 2567 (2013).
- [30] P.P. Chakrabarty, S. Saha, D. Schollmeyer, A.K. Boudalis, A.D. Jana, D. Luneau. *J. Coord. Chem.*, **66**, 9 (2013).
- [31] M.N.H. Irving, R.M. Parkins. *J. Inorg. Nucl. Chem.*, **27**, 270 (1965).
- [32] (a) COSMO. *Version 1.60*, Bruker AXS Inc., Madison, WI (2005); (b) SAINT. *Version 7.06A*, Bruker AXS Inc., Madison, WI (2005); (c) SADABS. *Version 2.10*, Bruker AXS Inc., Madison, WI (2005).
- [33] M.C. Burla, R. Caliendo, M. Camalli, B. Carrozzini, G.L. Casciaro, L. De Caro, C. Giacovazzo, G. Polidori, R. Spagna. *J. Appl. Crystallogr.*, **38**, 381 (2005).
- [34] G.M. Sheldrick. *SHELXL-97*, University of Göttingen, Göttingen (1997).
- [35] M. Amanlou, S.D. Siadat, S.E. Ebrahimi, A. Alavi, M.R. Aghasadeghi, M. Shafiee Ardestani, S. Shانهsaz, M. Ghorbani, B. Mehraei, M. Shafiee Alavideh, A. Jabbari-Arabzadeh, M. Abbasi. *Int. J. Nanomedicine*, **6**, 747 (2011).
- [36] M.C. Estévez, M.B. O'Donoghue, X. Chen, W. Tan. *Nano Res.*, **2**, 448 (2009).
- [37] Hypercube Incorporation. *HyperChem(TM) Professional 8.0*, Hypercube, Inc., Gainesville, FL (2007).
- [38] S. Forli. *Raccoon AutoDock VS: an automated tool for preparing AutoDock virtualScreenings*, Available from <http://autodock.scripps.edu/resources/raccoon>.
- [39] M. Kasuno, M. Hayano, M. Fujiwara, T. Matsushita. *Polyhedron*, **28**, 425 (2009).
- [40] R.K. Boggess, J.W. Hughes, W.M. Coleman, L.T. Taylor. *Inorg. Chim. Acta*, **38**, 183 (1980).
- [41] P. Kar, M.G.B. Drew, A. Ghosh. *Inorg. Chim. Acta*, **405**, 349 (2013).
- [42] S. Mandal, T.K. Karmakar, A. Ghosh, M. Fleck, D. Bandyopadhyay. *Polyhedron*, **30**, 790 (2011).
- [43] H. Ihtshamul, J. Ladbury. *J. Mol. Recog.*, **13**, 188 (2000).
- [44] M.A. Vázquez-Fernández, M.I. Fernández-García, G. González-Riopiedre, M. Maneiro, M.J. Rodríguez-Doutón. *J. Coord. Chem.*, **64**, 3843 (2011).
- [45] J.P. Costes, F. Dahan, B. Donnadiou, M.I. Fernandez-Garcia, M.J. Rodriguez-Douton. *Dalton Trans.*, 3776 (2003).

- [46] A. Srishailam, Y.P. Kumar, P. Venkat Reddy, N. Nambigari, U. Vuruputuri, S.S. Singh, S. Satyanarayana. *J. Photochem. Photobiol. B*, **132**, 111 (2014).
- [47] Y. Zhang, X. Wang, W. Fang, X. Cai, F. Chu, X. Liao, J. Lu. *Bioinorg. Chem. Appl.*, **2013**, Article ID 437134, 14 pages (2013). doi:[10.1155/2013/437134](https://doi.org/10.1155/2013/437134).
- [48] A.K. Boudalis, J.M. Clemente-Juan, F. Dahan, J.P. Tuchagues. *Inorg. Chem.*, **43**, 1574 (2004).
- [49] C.Y. Zhou, J. Zhao, Y.B. Wu, C.X. Yin, Y. Pin. *J. Inorg. Biochem.*, **101**, 10 (2007).
- [50] N. Raman, S. Sobha. *Spectrochim. Acta, Part A*, **85**, 223 (2012).
- [51] V. Kettmann, D. Košťálová, H.D. Höltje. *J. Comput. Aided Mol. Des.*, **18**, 785 (2004).
- [52] R. Corradini, S. Sforza, T. Tedeschi, R. Marchelli. *Chirality*, **19**, 269 (2007).
- [53] P. Heffeter, U. Jungwirth, M. Jakupec, C. Hartinger, M. Galanski, L. Elbling, M. Micksche, B. Keppler, W. Berger. *Drug Resist. Update.*, **11**, 1 (2008).
- [54] P.J. Dyson, G. Sava. *Dalton Trans.*, 1929 (2006).